Science of the Total Environment 627 (2018) 985–996

Contents lists available at ScienceDirect

Science of the Total Environment

journal homepage: www.elsevier.com/locate/scitotenv

Dry-wet cycles of kettle hole sediments leave a microbial and biogeochemical legacy

Florian Reverey [a,e,*], Lars Ganzert [c], Gunnar Lischeid [a,e], Andreas Ulrich [b], Katrin Premke [d], Hans-Peter Grossart [c,f]

[a] Leibniz Centre for Agricultural Landscape Research, Working Group: Small Water Bodies in Agricultural Landscapes, Eberswalder Str. 84, 15374 Müncheberg, Germany
[b] Leibniz Centre for Agricultural Landscape Research, Working Group: Microbial Biogeochemistry, Eberswalder Str. 84, 15374 Müncheberg, Germany
[c] Leibniz-Institute of Freshwater Ecology and Inland Fisheries, Department of Experimental Limnology, Alte Fischerhütte 2, OT Neuglobsow, 16775 Stechlin, Germany
[d] Leibniz-Institute of Freshwater Ecology and Inland Fisheries, Department of Chemical Analytics and Biogeochemistry, Müggelseedamm 310, 12587 Berlin, Germany
[e] Potsdam University, Institute of Earth and Environmental Science, Karl-Liebknecht-Str. 24-25, 14476 Potsdam-Golm, Germany
[f] Potsdam University, Institute for Biochemistry and Biology, Maulbeerallee 2, 14469 Potsdam, Germany

HIGHLIGHTS

- Dry-wet cycling leaves a microbial and biogeochemical legacy in kettle hole sediments.
- The legacy is driven by redox conditions, pH and organic matter properties.
- Carbon mineralization peaks in dry sediments with a less stable hydrological past.
- Nitrogen loss is potentially highest in hydrologically less stable sediments.

GRAPHICAL ABSTRACT

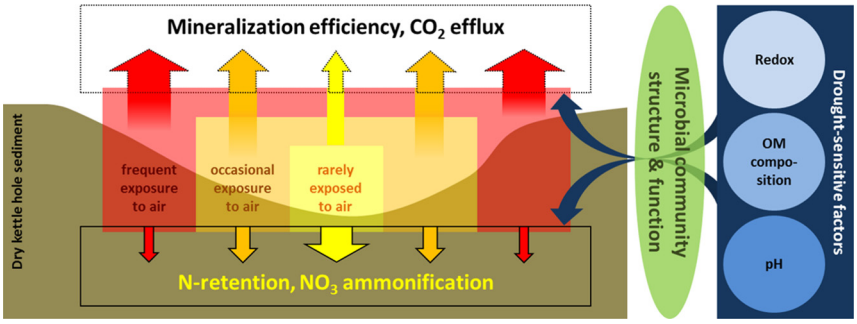

ARTICLE INFO

Article history:
Received 3 November 2017
Received in revised form 20 January 2018
Accepted 22 January 2018
Available online 3 February 2018

Editor: F.M. Tack

Keywords:
Desiccation
DNRA
Denitrifiers
Organic matter mineralization
Carbon
Nitrogen

ABSTRACT

Understanding interrelations between an environment's hydrological past and its current biogeochemistry is necessary for the assessment of biogeochemical and microbial responses to changing hydrological conditions. The question how previous dry-wet events determine the contemporary microbial and biogeochemical state is addressed in this study. Therefore, sediments exposed to the atmosphere of areas with a different hydrological past within one kettle hole, i.e. (1) the predominantly inundated pond center, (2) the pond margin frequently desiccated for longer periods and (3) an intermediate zone, were incubated with the same rewetting treatment. Physicochemical and textural characteristics were related to structural microbial parameters regarding carbon and nitrogen turnover, i.e. abundance of bacteria and fungi, denitrifiers (targeted by the *nirK* und *nirS* functional genes) and nitrate ammonifiers (targeted by the *nrfA* functional gene). Our study reveals that, in combination with varying sediment texture, the hydrological history creates distinct microbial habitats with defined boundary conditions within the kettle hole, mainly driven by redox conditions, pH and organic matter (OM) composition. OM mineralization, as indicated by CO_2-outgassing, was most efficient in exposed sediments with a less stable hydrological past. The potential for nitrogen retention via nitrate ammonification was highest in the hydrologically rather stable pond center, counteracting nitrogen loss due to denitrification. Therefore, the degree of hydrological stability is an important factor leaving a microbial and biogeochemical legacy, which determines carbon and nitrogen losses from small lentic freshwater systems in the long term run.

* Corresponding author at: Leibniz Centre for Agricultural Landscape Research, Working Group: Small Water Bodies in Agricultural Landscapes, Eberswalder Str. 84, 15374 Müncheberg, Germany.
E-mail address: reverey@zalf.de (F. Reverey).

https://doi.org/10.1016/j.scitotenv.2018.01.220

1. Introduction

A changing climate with an increased likelihood of extreme events such as high temperature periods or precipitation events has been forecasted for the near future (Fischer and Knutti, 2015). Therefore, the hydrology and physicochemistry of global freshwater systems is expected to become more dynamic and variable, increasing the occurrence of semi-aquatic environments with intermittent stages (i.e. drying and rewetting).

Sequences of inundation and desiccation come along with changes in physicochemical conditions (i.e. redox potential, pH), organic matter (OM) and nutrient (e.g. nitrogen) availability (Reverey et al., 2016). This increased variability will have profound consequences for the ecosystem's microbial community structure and functioning and thus gear cascades of biogeochemical responses. For example, the OM turnover rate in kettle holes was found to be enhanced in systems with a temporal hydroperiod (Nitzsche et al., 2017). Thus, frequent dry-wet cycles of sediments are hypothesized to boost loss of previously stored carbon (C) to the atmosphere. Accordingly, increased CO_2 emissions were measured in desiccated temporary streambeds (Gómez-Gener et al., 2016). Further, CO_2 outgassing in temporary ponds was shown to be highest in OM-rich sediments that were repeatedly exposed to the atmosphere (Catalan et al., 2014), and incubations of littoral lake sediment revealed that dry treatments released significantly more CO_2 than wet controls (Weise et al., 2016).

Whereas it seems that organic carbon is preferentially released from drying sediment, the question remains whether nitrogen is lost or retained in the system. This uncertainty is mainly due to the fact that nitrogen (N) dynamics in sediments are determined by a complex interplay between different N transformation processes. For example, coupled nitrification and denitrification will lead to N outgassing, whereas dissimilatory nitrate reduction to ammonium (DNRA) can compete with denitrification, and thus retains N in the system (Burgin and Hamilton, 2007). These different processes all depend on redox states and fluctuations, as induced by dry-wet cycles. It has been shown that, for example, microbial communities responsible for nitrogen transformations in wetland ecosystems readjust their structural and functional equilibrium as a consequence of repeated moisture and hence redox fluctuations (Peralta et al., 2013).

In this study, we consider stress to be a change in environmental conditions (e.g. drought) that triggers a physiological response threatening microbial functioning or survival (according to Schimel et al., 2007). Subsets of the microbial communities are able to tolerate the above-mentioned temporal dynamics, whereas others with more restricted physiological flexibility will be more sensitive to local disturbance (DeAngelis et al., 2010; Schimel et al., 2007). Basically, strategies of microorganisms to deal with such environmental stress include resistance or resilience mechanisms, which can be on the functional level and reversible or on the structural level, inducing the shift to a new equilibrium different from the initial state (Barthès et al., 2015). Whether loss of stress susceptible microbial species changes the community's functional traits or is compensated for by functional replacement with other taxa greatly depends on the degree of specialization of the lost species (Peralta et al., 2013) as well as on the biodiversity of the functional group, potentially buffering loss of individual species (Peralta et al., 2014). Drying and rewetting can lead to enrichment or depletion of specific compounds such as OM or nutrients and thus influence microbial activity, which does not necessarily coincide with a change in microbial community structure. The magnitude of microbial responses greatly depends on the duration and frequency of environmental changes, i.e. of drought or flood events. Short-term events will impact biogeochemistry on the process level, but might not change microbial community structure, whereas long-term events or a high frequency of short-term events can exert a much stronger selective pressure on microorganisms prone to stress (Fig. 1; Reverey et al., 2016). Consequently, adaptation of microorganisms to dry-wet cycling strongly depends on the sediment's hydrological history. For example, the microbial community was hypothesized to preadapt to a certain degree of moisture fluctuation, whereas extreme events outside an environment's historical range of variability lead to stronger functional and structural responses (Evans and Wallenstein, 2011). In soil incubation experiments, a soil microbial community was enriched mainly consisting of taxa that were more active under fluctuating than static redox conditions (DeAngelis et al., 2010). However, a change in microbial functioning and community structure in lake sediments was only observed after exposure to extended drought events (Weise et al., 2016). Historical preadaptation can form a microbial community which is more efficient regarding specific transformation processes. For example, the stimulus of microbial potentials upon rewetting of dry pond sediments was observed to be higher with frequent exposure to dry-wet cycling than with shorter and/or infrequent dry phases (Fromin et al., 2010).

Kettle holes are small, glacially created ponds, which generally have a highly variable hydroperiod (Kalettka and Rudat, 2006), leading to frequent dry-wet cycles and thus represent excellent model systems for our study. The question how variations in the duration and frequency of previous drought events impact sediment C and N losses to the atmosphere has been addressed by comparing selected biogeochemical and microbial variables between sediment areas with a different hydrological past within the same kettle hole. We hypothesize that prolonged drought increases sediment C and N losses due to increased OM mineralization, and decreases sediment C and N retention. Furthermore, the hydrological past of the sediment, i.e. the duration and frequency of previous dry-wet events, is suggested to determine future biogeochemical processes and microbial community structure by changing physicochemical boundary conditions such as water content, pH and OM composition.

2. Methods

2.1. Study site

The study site is located in the Quillow catchment (168 km^2) in North-East Brandenburg, Germany. The hummocky, young moraine landscape is coined by small, glacially created depression wetlands that are characterized by a highly variable hydroperiod. This variability is driven by water inputs mainly due to precipitation, snow melt, interflow, shallow groundwater discharge and surface runoff as well as water loss due to evapotranspiration, lateral subsurface flow, and shallow groundwater recharge (Reverey et al., 2016).

The kettle hole "Rittgarten" (N 53°23′22″ E 013°42′09″) is situated in the Uckermark region, mainly consisting of sandy soils (Kleeberg et al., 2016). The climate is sub-humid, with a mean annual temperature of 9.1 °C and a mean annual precipitation of 561 mm in 2015 (Nitzsche

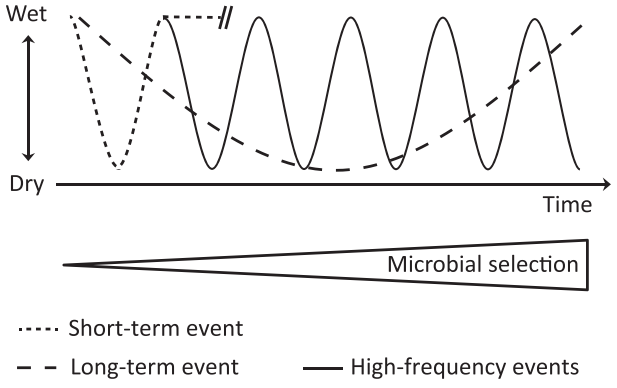

Fig. 1. Potential effect of different scenarios of dry-wet cycling on the degree of microbial selection.

et al., 2017). The kettle hole basin has an area of 1453 m^2, and its water depth ranges between 0 and 2.3 m, indicating its temporary character: In 2015, it was inundated from the beginning of the year until May, whereupon it dried out progressively and was completely exposed to the atmosphere in October.

2.2. Sampling

Sampling took place at 12th and 13th of October 2015, when the kettle hole sediment was completely exposed to the atmosphere. This gave us the opportunity to sample sediment from regions with a different hydrological background (in the following named zones A–C) within one system:

1. Zone A: The area including the deepest point, which has been permanently inundated for at least the last five years and was then exposed to the atmosphere for one month prior to sampling.
2. Zone B: An intermediate zone including two distinct points 30 cm above the deepest point, which is occasionally falling dry and has been exposed for 3 months prior to sampling.
3. Zone C: A marginal zone including two distinct points 60 cm above the deepest point, which is very frequently exposed to dry-wet cycling and has been exposed for 5 months prior to sampling.

Sampling followed a transect of five sampling points through these zones. Four replicates were taken from each point (Fig. 2).

Sediment for physicochemical analysis and organic matter properties was sampled using a PE tube (∅ 7 cm) which was pushed vertically into the ground. The first 5 cm were sliced off, homogenized and subsequently stored on ice for transport to the lab. For molecular biological analysis, ca. 0.3 g of the homogenized sediment where filled into 2 mL Eppendorf tubes, stored on dry ice for transport and subsequently frozen at −80 °C.

Additional cores were taken from each sampling point in quadruplicates for gas measurements and further incubations (see 2.3) with 10 cm of sediment from each point pushed into PE incubation tubes (∅ 5.4 cm, height 30 cm).

2.3. Incubation of sediment cores

Incubation cores were placed in a climate chamber (20 °C, 100% humidity) in the dark to prevent photosynthesis and autotrophic respiration. Initial incubation was done without water addition as an open system. However, biogeochemical responses to dry-wet cycles also depend on the sediment state, i.e. whether the sediment is exposed to the atmosphere or inundated. In order to consider potential effects in both states, an inundated phase was included. Therefore, a 10 cm column of artificial lake water, according to Fabian et al. (2017), was poured carefully onto the sediment after ten days of exposed incubation. Thereby, a sediment layer of 10 cm, a water column of initially 10 cm, and a headspace of 5 cm was created. Ambient air was constantly bubbled through the supernatant water to keep gas concentrations in equilibrium with the atmosphere. Flushing was only interrupted during gas measurements (see 2.5). After rewetting, the sediment was incubated for another 36 days as an open system. Subsequently, the upper 5 cm of the sediment were sliced off, homogenized and frozen at −20 °C for further physicochemical analysis and organic matter properties. For molecular biological analysis, ca. 0.3 g of the homogenized sediment were filled into 2 mL Eppendorf tubes and directly frozen at −80 °C.

2.4. Physicochemical analysis

Sand, silt and clay contents were determined according to ISO 11277. Sediment moisture was determined by subtracting the weight of freeze-dried sediment from its wet weight. The dry sediment was combusted in a muffle furnace at 550 °C for 4 h to estimate the organic matter (OM) content by subtracting the ash weight from the dry weight (loss on ignition).

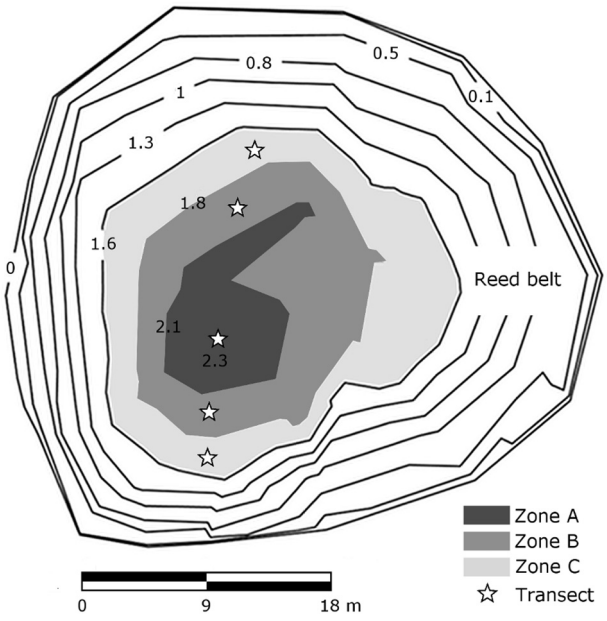

Fig. 2. Bathymetric map of the kettle hole Rittgarten, including zones A–C (grey shadings) and the transect through the zones (stars). Contour lines represent depth (m) below reference.

Total carbon (TC) and nitrogen (TN) were measured with a TruSpec elementary analyzer (Leco Instruments GmbH). Total organic carbon (TOC) was obtained via fractionated simultaneous determination with a RC612 multiphase carbon and water analyzer (Leco Instruments GmbH). Mineral nitrogen (NH_4^+ and NO_3^-) was extracted with potassium chloride (KCl) and measured with a CFA-SAN spectrophotometer ($Skalar_{analytic}$ GmbH). The pH value was determined via water extraction according to ISO 10390.

2.5. Gas measurements

For gas measurements, incubation cores were closed using a gas tight lid. The lid was equipped with an in- and outlet for connecting an Ultraportable Greenhouse Gas Analyzer (UGGA; Los Gatos Research, Inc., USA), thus creating a closed loop including the headspace in the incubation tube. CO_2 and CH_4 concentration in the headspace (ppm) were measured directly after closing the lid (t_0) and after 6 h (t_1). For these measurements, the UGGA was connected for approximately 3 min until the gas concentration in the loop reached a plateau.

The amount of carbon in the headspace and the supernatant water C_{gas} (g C) was calculated according to formula 1. The daily net gas production rate Net_{gas} (g C m^{-2} d^{-1}) was determined by using formula 2. Gas measurements followed the scheme given in Table 1.

$$C_{gas} = \left(10^{-6}\frac{P * c * V_{hs}}{R * T} + \frac{c * k_H * V_{sn}}{1000}\right)M \quad (1)$$

where P is the atmospheric pressure (atm), c is the respective gas concentration in the headspace (ppm), V_{hs} is the headspace volume, R is the gas constant (m^3 Pa K^{-1} mol^{-1}), T is the temperature (K), k_H is Henry's constant (mol L^{-1} atm^{-1}) adjusted for temperature (Goldenfum, 2010), V_{sn} is the volume of supernatant water and M is the molar mass of carbon.

$$Net_{gas} = \frac{C_1 - C_0}{t * A} * 24 \quad (2)$$

where C_1 is C_{gas} at t_1, C_0 is C_{gas} at t_0, t is the incubation time during the gas measurements (6 h), A is the area of the incubation cores (m^2) and the last term converts hours to days.

Cumulated gas-efflux was calculated as the sum of all Net_{gas} for each core (see Table 1).

Mineralization efficiency (E_M) (μg C g^{-1} TOC d^{-1}) was calculated according to formula 3.

$$E_M = \frac{C_{gas} * 10^6}{TOC} \quad (3)$$

where TOC is the amount of total organic carbon in the incubation core.

2.6. Organic matter properties

The mobile and biologically easily available part of total sediment organic matter (OM) is reflected in the water extractable organic matter pool (WEOM). Freeze-dried and ground sediment was shaken (100 rpm, 4 °C) with deionized water (sediment:water ratio of 1:10) for 48 h, according to Gómez-Gener et al. (2016), and the leachate was filtered over PES filters (0.2 μm). Dissolved organic carbon (DOC) of the leachate was measured with a Total Organic Carbon Analyzer (Shimadzu TOC-V CPH). Dissolved OM (DOM) quality was analyzed by UV/Vis absorbance and fluorescence spectra of the WEOM extracts, with the extracts being diluted to a DOC content of approximately 10 mg L^{-1} (Anesio et al., 2000).

UV/Vis absorbance (200–800 nm) was measured spectrophotometrically with a Hitachi U-2900 using a 1 cm quartz cuvette. The specific UV absorption at 254 nm (SUVA), which is positively correlated to DOM aromaticity and usually ranges between 1 and 9 L mg^{-1} m^{-1} (Weishaar et al., 2003), was determined by dividing the absorbance at 254 nm by the DOC concentration of the extracts (mg L^{-1}) and the cuvette path length (0.01 m).

Fluorescence excitation-emission matrixes (EEM) were measured (Hitachi F-7000 Fluorescence Spectrophotometer) using a 1 cm quartz cuvette. The emission range of the EEM scans ranged from 270 to 630 nm with 1 nm increments, the excitation range was 240–400 nm with 10 nm increments. Additionally, blank measurements were done with Milli-Q Millipore water. Spectral correction, inner filter correction, Raman normalization and blank subtraction of the EEM's were conducted according to Murphy et al. (2010). Three indices were calculated: The Fluorescence Index (FIX), the Biological Index (BIX) and the Humification Index (HIX). FIX indicates terrestrial versus autochthonous origin of the OM (low versus high values, respectively) and is the ratio of the emission intensities at 470/520 nm at an excitation wavelength of 370 nm (Cory and McKnight, 2005). BIX refers to DOM origin and freshness, where high values indicate freshly produced autochthonous DOM, while low values correspond to a lower recent autochthonous contribution; it is calculated as the ratio of the emission intensities at 380/430 nm at an excitation wavelength of 310 nm (Huguet et al., 2009). HIX is positively correlated with the degree of humification and is the ratio between the two spectral areas spanning between emission intensities of 435–480 nm and 300–345 nm at an excitation wavelength of 254 nm (Huguet et al., 2009; Zsolnay et al., 1999).

2.7. DNA extraction

DNA was extracted according to Nercessian et al. (2005) with some modifications. Briefly, 0.3 g sediment sample (wet weight) with 0.1 mm and 0.7 mm zirconia-silica beads plus 4 glass beads (3 mm) were suspended in 600 μL of extraction buffer (10% CTAB in 1.6 M NaCl mixed 1:1 with 240 mM potassium phosphate buffer) plus each 60 μL of 10% sodium dodecyl sulfate (SDS) and 10% N-lauroyl sarcosine. After the addition of 600 μL phenol-chloroform-isoamyl alcohol (25:24:1), samples were homogenized by bead beating on a vortexer (10 min at 2850 rpm) and subsequently centrifuged at 16000 ×*g* for 10 min at 4 °C. The aqueous phase was transferred into a new Eppendorf tube and mixed with an equal volume of chloroform-isoamyl alcohol (24:1) and centrifuged at 16000 ×*g* for 10 min at room temperature. The upper phase was then mixed with 2 volumes of 30% PEG 6000 in 1.6 M NaCl and incubated at 4 °C for 1.5 h. Afterwards, the mixture was centrifuged at 17000 ×*g* for 60 min at 4 °C and the aqueous phase was discarded. The resulting pellet was washed with 1 mL ice-cold ethanol (70%), dried briefly at 37 °C and re-suspended in 50 μL DEPC-treated water.

2.8. Realtime PCR

Quantitative PCR was performed on an ABI 7500 Fast real-time PCR System (Applied Biosystems) using the Kapa Sybr® Fast qPCR Kit. Each 20 μL reaction mixture contained 10 μL of the Kapa Sybr® Fast Master Mix (2×) Universal, a final concentration of 200 nM of each forward and reverse primer (Table S1), 0.4 μL of ROX Low and 2 μL of

Table 1
Measurement scheme for the incubation cores: After ten days, cores exposed to the atmosphere were rewetted and stayed inundated until the end of the experiment. All physicochemical and biological parameters were collected at days 1 and 46, except gas measurements that were conducted throughout the incubation period (as indicated by "X").

Day		1	5	11	16	21	26	32	46
Condition		Exp[a]	Exp[a]	Ind[b]	Ind[b]	Ind[b]	Ind[b]	Ind[b]	Ind[b]
CO_2	*Daily net CO_2 production ($gC\ m^{-2}\ d^{-1}$)*	X	X	X	X	X	X	X	X
CH_4	*Daily net CH_4 production ($mgC\ m^{-2}\ d^{-1}$)*	X	X	X	X	X	X	X	X
E_M	*Mineralization efficiency ($\mu gC\ gTOC^{-1}\ d^{-1}$)*	X							X
TC/TOC/TN	*Total carbon, organic carbon and nitrogen fraction (%)*	X							X
NO_3^-/NH_4^+	*Nitrate and ammonium content ($mg\ kg^{-1}$)*	X							X
pH	*pH value*	X							X
SO_4^{2-}	*Sulfate content ($g\ kg^{-1}$)*	X							X
Sand/Silt/Clay	*Sand, silt and clay fraction (%)*	X							
OM	*Organic matter content (%)*	X							X
WC	*Water content*	X							X
SUVA	*Specific UV-absorption (254 nm) ($L\ mg^{-1}\ m^{-1}$) of WEOM*	X							X
BIX	*Biological index of WEOM*	X							X
HIX	*Humification index of WEOM*	X							X
FIX	*Fluorescenc index of WEOM*	X							X
16S	*Bacterial abundance (16S rRNA gene copies $ngDNA^{-1}$)*	X							X
18S	*Fungal abundance (18S rRNA gene copies $ngDNA^{-1}$)*	X							X
Denitrifiers	*nirS and nirK fraction (% 16S)*	X							X
Nitrate ammonifiers	*nrfA fraction (% 16S)*	X							X

[a] Exposed to the atmosphere.
[b] Inundated.

template DNA (final concentration of <20 ng). To enhance PCR efficiency, 0.4 μL of bovine serum albumin (BSA, 30 mg mL^{-1}) was added to each reaction mixture. The activation step for each primer pair was 3 min at 95 °C. For *nirS* and *nirK*, the protocol of Henry et al. (2004) was slightly modified, starting with six touchdown cycles with 15 s at 95 °C, 30 s at 63 °C for annealing and 45 s at 72 °C; annealing temperature was decreased by 1 °C each cycle. These were followed by 40 cycles with the same conditions, except for using an annealing temperature of 58 °C. The conditions for the *nrfA* assay were according to Song et al. (2014), with a few modifications: 50 cycles including 15 s at 95 °C, 45 s at 52 °C for annealing and 1 min at 72 °C. Bacterial 16S and fungal 18S rRNA genes were amplified according to Zeleke et al. (2013) and Becker et al. (2014), respectively. Gene copy numbers were detected in duplicates. The standard curves were obtained by serial dilutions of genomic DNA from *Pseudomonas putida* F1 (for bacteria) or *Escherichia coli* C600 (for nitrate ammonifiers) or plasmid DNA harboring a respective gene fragment for the other assays (Becker et al., 2014). 16S rRNA gene copy numbers were calculated based on the genome size and the number of 16S rRNA genes present in *Pseudomonas putida* F1. Serial dilutions of the sediment samples were used to prove equal PCR efficiency of standard and samples. PCR efficiencies ranged between 87 and 97%.

The abundance of each functional gene was standardized by dividing the copy number by the 16S rRNA gene copy number. In order to estimate the relative importance of denitrification and nitrate ammonification, the ratio of nitrite reductases (RatioNR) was calculated according to formula 4:

$$RatioNR = \frac{nirS + nirK}{nrfA} \quad (4)$$

where *nirS*, *nirK* (both denitrification) and *nrfA* (nitrate ammonification) represent copy numbers of the respective functional genes.

2.9. Community structure of nitrate ammonifiers (DNRA)

The community structure of nitrate ammonifiers was studied by determining length polymorphisms of the *nrfA* gene. PCR conditions were as previously described for the real-time PCR assay, except that the forward primer was fluorescently labeled with 6-FAM. Amplicons were purified with a MSB Spin PCRapace kit (Invitek), mixed with 0.2 μL ROX-labeled MapMarker 1000 (BioVentures) and subsequently separated on an AB 3500 genetic analyzer using POP-7 polymer (Applied Biosystems). It is well-known that due to the differing purine contents (Kaplan and Kitts, 2003), the separation of DNA fragments depends on their size as well as their nucleotide composition. In total, 34 DNA fragments with a size ranging between 220 and 280 bp were obtained for the *nrfA* amplicon. The profiles were analyzed using the GeneMapper software v. 5.0 and standardized in a similar manner as suggested by Dunbar et al. (2001).

2.10. Data analysis

All significance tests and the principal component analysis (PCA) were conducted with R version 3.1.2 using the packages *stats* (R Core Team, 2014), *dunn.test* (Dinno, 2016) and *ade4* (Dray and Dufour, 2007).

For each measured parameter (Table 1), significance of differences between zones within the sediment state (exposed or inundated) was tested applying a Kruskal-Wallis test. If significant, Dunn's test of multiple comparisons using rank sums was chosen as a posthoc test. Furthermore, we performed Mann-Whitney *U* tests to test differences between the exposed and inundated state within each zone.

To ordinate the three zones under exposed and inundated conditions by their biogeochemical properties (descriptors according to Table 1), we performed a PCA. All descriptors were then correlated with the respective principal components. Correlations with an R^2 <0.2 are not shown in the plots.

Changes in DNRA community structure were analyzed by nonmetric multidimensional scaling (NMDS) analysis. The relative proportion of the different *nrfA* amplicons was used as input for calculating NMDS by PC-ORD v.7.0 (McCune and Mefford, 2015). The presented NMDS analysis was performed using Bray-Curtis distance measure. The stress value was at 13.5 for a two-dimensional solution indicating a reliable test performance. Pearson product-moment correlations were calculated between the NMDS scores and chemical parameters of samples. Parameters showing significant correlation ($p < 0.05$) with at least one NMDS axis were included as vectors in the ordination plot. Significant differences in community structure between zones were tested by means of the Multi-Response Permutation Procedure (MRPP) as described previously (Felsmann et al., 2015). Matrix comparisons of the NMDS scores and the PCA scores were conducted using a Mantel test (number of permutations = 9999).

3. Results

3.1. Water content

Initial water content in zones A (inner zone) and B (intermediate zone) was 80.3 ± 2.2 (mean ± standard deviation) and 80.1 ± 3.2%, respectively, and did not increase significantly after rewetting (82.5 ± 3.6 and 82.9 ± 1.8%, respectively). In zone C (outer zone), the initial water content (62.5 ± 5.4%) increased significantly after rewetting (70.4 ± 3.6%) and was significantly lower than in zones A and B after as well as prior to rewetting.

3.2. Carbon turnover

The cumulation of the net CO_2– and CH_4-production (Net_{CO2} and Net_{CH4}, respectively) for each replicate showed highest CO_2-effluxes in zones B and C and lowest CO_2-effluxes in zone A, whereas CH_4-effluxes did not differ significantly between the zones (Fig. 3a).

Mineralization efficiency (E_M), i.e. the amount of C respired relative to the amount of TOC in the sediment, during exposed conditions was significantly higher in zone C than in zones A and B. During inundated conditions, there was no significant difference between the zones. However, E_M significantly dropped in all zones (A–C) during inundated conditions (Fig. 3b).

3.3. Organic matter source

In zone C, OM had a significantly higher degree of humification than in the moister zones A and B, as indicated by a higher humification index (HIX) of the water extractable organic matter (WEOM) under exposed and inundated conditions. In the exposed state, zones A and B exhibited a more recent autochthonous contribution to the OM pool than zone C, as indicated by a higher biological index (BIX) of the WEOM. In the inundated state, BIX values dropped significantly in all zones, but did not differ significantly from each other (Fig. 4). Further values of measured indices are given in the supplementary (Table S3).

3.4. Mineral nitrogen

During exposed conditions, nitrate concentration was significantly lowest in zone A and did not differ significantly between zones B and C. During inundated conditions, nitrate concentration did not differ significantly between the zones. In zones B and C, nitrate concentration decreased significantly after rewetting, whereas it did not change significantly in zone A (Fig. 5a). The opposite holds true for ammonium concentration: In the exposed state, it was highest in zone A, and zones B and C did not differ significantly from each other. Under inundated conditions, ammonium concentration was highest in zone A and lowest in zone C. After rewetting, it increased significantly in all three zones (Fig. 5b).

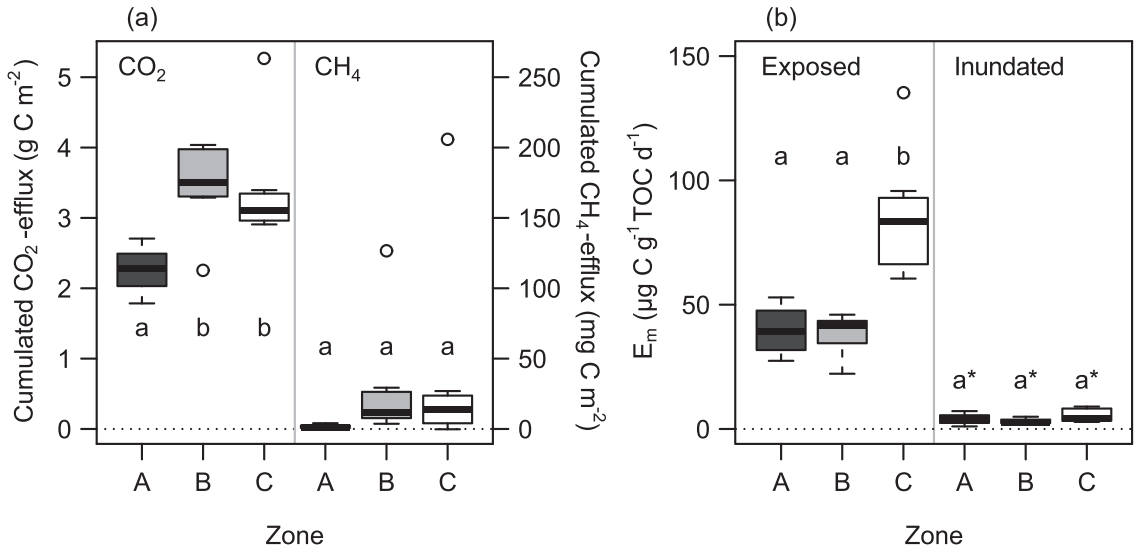

Fig. 3. (a) Cumulative CO_2 and CH_4 efflux, adding together all measurements for each replicate (no interpolation!). (b) Mineralization efficiency (E_M) during exposed and inundated conditions in the three different zones. Small letters indicate significance within each block separated by grey vertical lines; asterisks indicate significant effects of the treatment within zones.

3.5. Bacterial vs. fungal abundance

Results of the qPCRs are summarized in Table 2. Bacterial 16S rRNA gene copies neither differed significantly between zones nor between treatments. Fungal 18S rRNA gene copies showed a decreasing trend from exposed to inundated conditions, which was only significant in zone B. The overall trend of higher fungal abundance in zone B was non-significant. During inundated conditions, however, the 18S:16S ratio was significantly higher in zone B than in the other zones.

3.6. Denitrifiers and nitrate ammonifiers (DNRA)

Results of the qPCRs are summarized in Table 3. Abundance of the *nirS* gene did not differ between exposed and inundated conditions and was significantly lower in zone B compared to zones A and C. For *nirK*, abundance did not differ significantly between zones or treatments (i.e. exposed vs. inundated). However, there were trends (though not significant) towards lower values in zone B as well as higher values during inundated conditions in zones A and B. For *nrfA*, the trend of higher abundance in the inundated phase was significant in zone B. Zone A displayed the highest values of all zones.

The ratio between *nirS* and *nirK* did not differ significantly between zones during exposed conditions. Though differences between exposed and inundated conditions were not significant in all three zones, the ratio was higher in zone C than in zones A and B during inundated conditions (Fig. 6a). RatioNR was significantly lowest in zone A, driven by higher *nrfA* abundance, and highest in zone C during exposed and inundated conditions. RatioNR dropped significantly after rewetting in zones B and C, but did not change significantly in zone A (Fig. 6b).

Shifts in the community structure of nitrate ammonifiers were studied by length polymorphism of the *nrfA* gene. The first two dimensions of the resulting NMDS are shown in Fig. 7. Dimension 1 clearly separates zone C from zones A and B, whereas dimension 2 further disentangles zones A and B. Accordingly, the MRPP test revealed significant differences of the *nrfA* communities between the zones irrespective of the treatment (i.e. exposed vs. inundated) (A-values ranged from 0.26 to 0.4; all $p < 0.001$), except in zone A where the treatment showed a significant difference between the exposed and the inundated phase (A-value 0.21; $p = 0.015$). Correlations between abiotic descriptors and dimension 1 revealed that the DNRA community in zone C was mainly influenced by higher sand content and terrestrial, humic-like OM, as indicated by the humification index (HIX), whereas the communities in zone A and B were influenced by higher silt and clay content, water content and autochthonous OM, as indicated by the fluorescence index (FIX). Additionally, correlations of abiotic descriptors with dimension 2 indicated that the DNRA community in zone A differed from the one in zone B with a higher pH and lower TOC content.

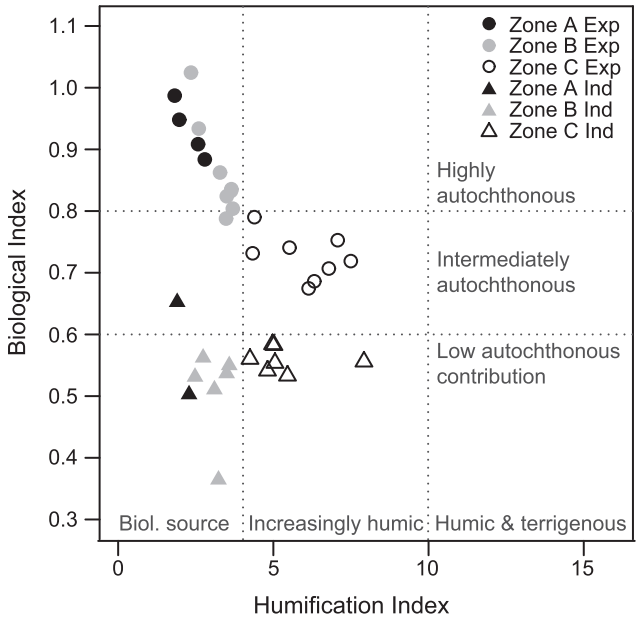

Fig. 4. Humification index (HIX) against Biological index (BIX) during exposed (Exp) and inundated (Ind) conditions for all three zones.

3.7. Multivariate ordination of the three kettle hole zones

The first three components of the PCA explained 71.6% of the total variance (Fig. 8). The first principal component (PC) (39.1% of total variance) clearly separated the inner zones A and B from the outer zone C and mainly correlated with sediment texture, C and N stocks, OM quantity and quality as well as water content. The second PC (22.8% of total

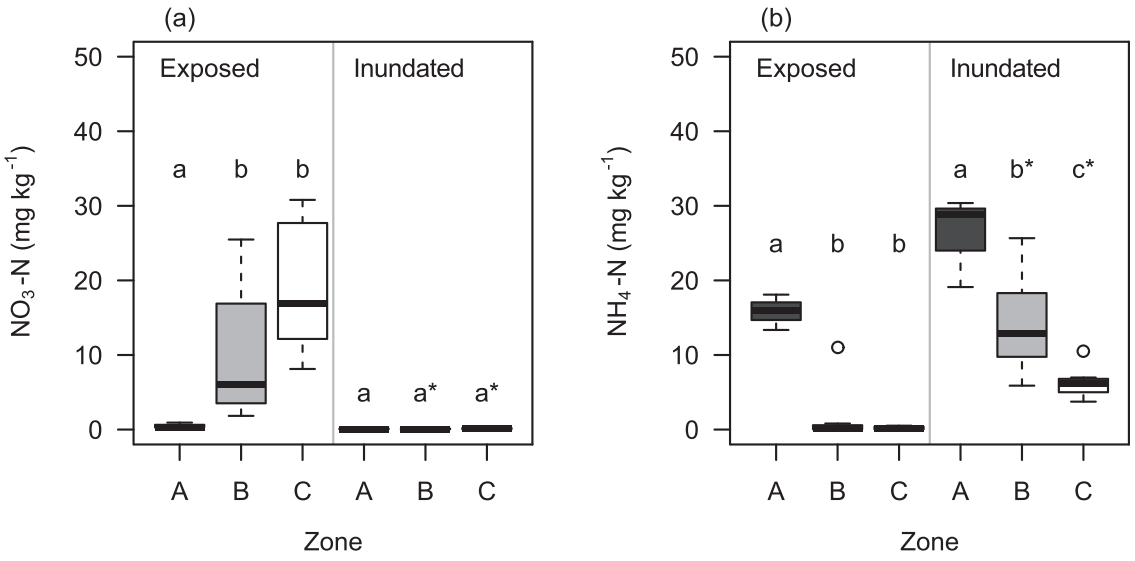

Fig. 5. Nitrate (a) and ammonium (b) concentrations during exposed and inundated conditions in the three different zones. Small letters indicate significance within treatment (separated by grey line); asterisks indicate significant effects of the treatment within zones.

variance) distinguished between exposed and inundated conditions, and mainly correlated with C-mineralization, fungal abundance, mineral N stocks, pH and OM freshness. The third PC (9.6% of total variance) separated the inner zones A and B, and was mainly correlated with abundance of bacteria containing genes for nitrite reductases (*nrfA*, *nirS* and *nirK*) as well as OM freshness. Matrix comparisons of the PCA scores and the NMDS scores revealed a positive correlation of principal components 1 and 3 (Fig. 8b) with NMDS dimensions 1 and 2 (Fig. 7) (Mantel test, $r = 0.4497$, $p = 0.0001$).

4. Discussion

Our investigations focusing on biogeochemical and microbial legacies left by dry-wet cycles in kettle hole sediments revealed clear differences in biogeochemistry and selected microbial variables between the different hydrological zones, which explained about 50% of the total variance (PC 1 and 3; Fig. 8b). As the zones included samples from distinct points with a similar hydrological history, it is suggested that biogeochemical differences between the zones are caused by varying patterns of previous dry-wet cycling (see 2.2). On the other side, about 20% of the total variance was explained by the dry-wet change during the incubation (PC 2, Fig. 8a). This variance is more likely to display microbial functional responses.

4.1. Boundary conditions

The most important factors for separation of the outer, drier zone C from the inner, moister zones A and B were physicochemical parameters such as water content, sediment texture as well as OM quantity and quality. Differences of sediment texture are presumably mostly related to the fact that fine sediment particles including silt, clay and fine OM particles tend to accumulate in the center due to the grading effect of fluviatile transport during inundation or heavy rain events. Furthermore, wind action can cause dust deposition, thus removing fine sediment particles from dry areas. This is reflected in the higher sand as well as lower silt, clay and OM content in the outer, driest zone C.

Water content in zones A and B did not change significantly after rewetting. Consequently, sediments from these zones are obviously water-saturated even during exposed conditions, at least during short-term periods. This is in accordance with typical water retention curves for clayey soils and sediments, i.e. the relationship between matrix potential (or water level height during periods of inundation) and water content (Hillel, 1980). Accordingly, reducing matrix potential from positive values (indicating inundation) to slightly negative values does not result in a marked decrease of water content, and correspondingly only slightly increases the air content in the sediment pores (Reiche et al., 2009; Knorr et al., 2008). On the contrary, rewetting significantly increased the moisture of the more sandy sediments from

Table 2
Bacterial and fungal abundance ± standard deviation as determined by 16S and 18S rRNA gene copies in sediment DNA extracts. The symbols in the last three rows indicate significant differences between zones ("−": not significant; "+": $p < 0.05$). Bold numbers indicate a significant difference between the respective and the other two zones. Asterisks indicate significant differences between states (exposed vs. inundated) within a zone ("*": $p < 0.05$).

	Exposed			Inundated		
Zone	**16S** *Copies ngDNA^{-1} (*1000)*	**18S** *Copies ngDNA^{-1} (*1000)*	**18S:16S**	**16S** *Copies ngDNA^{-1} (*1000)*	**18S** *Copies ngDNA^{-1} (*1000)*	**18S:16S**
A	187.9 ± 20.7	4.2 ± 1.4	0.02 ± 0.007	187.8 ± 35.0	2.3 ± 0.9	0.01 ± 0.002
B	195.4 ± 37.9	7.9 ± 4.5*	0.03 ± 0.012	180.8 ± 52.7	3.6 ± 0.6*	**0.02 ± 0.005**
C	235.5 ± 168.3	4.6 ± 3.6	0.02 ± 0.012	165.5 ± 50.1	2.4 ± 1.4	0.01 ± 0.005
A:B	−	−	−	−	−	+
A:C	−	−	−	−	−	−
B:C	−	−	−	−	−	+

Table 3
Abundance of functional genes for denitrifiers (*nirS* and *nirK*) and nitrate ammonifiers (*nrfA*) ± standard deviation in sediment samples. Gene copy numbers were calculated as relative proportions using the respective bacterial 16S rRNA copy number. The symbols in the last three rows indicate significance of differences between zones or between states ("−": not significant; '+': $p < 0.05$; "++": $p < 0.01$). Bold numbers indicate a significant difference between the respective and the other two zones. Asterisks indicate significant differences between states (exposed vs. inundated) within a zone ('*': $p < 0.05$).

	Exposed			Inundated		
Zone	***nirS***	***nirK***	***nrfA***	***nirS***	***nirK***	***nrfA***
	% 16S	*% 16S*	*% 16S*	*% 16S*	*% 16S*	*% 16S*
A	8.9 ± 2.5	15.7 ± 14.6	12.7 ± 11.6	5.9 ± 1.8	27.1 ± 3.7	**18.2 ± 3.1**
B	**1.5 ± 0.7**	6.7 ± 11.4	2.0 ± 3.3*	**1.6 ± 1.1**	13.4 ± 10.0	4.7 ± 3.4*
C	6.1 ± 5.1	16.2 ± 19.0	2.3 ± 1.6	8.0 ± 3.2	15.3 ± 13.1	5.0 ± 4.3
A:B	++	−	+	+	−	+
A:C	−	−	−	−	−	+
B:C	+	−	−	++	−	−

zone C, indicating a drying effect. Besides the abovementioned relationship, this can also be explained by the fact that zone C has been exposed to the atmosphere for the longest period (5 months prior to sampling). Therefore, we assume that being exposed to the atmosphere increases the redox potential only at the sediment surface in the moister zones A and B, whereas in the drier zone C oxygen may have been enriched even in deeper layers due to the higher sand and increased air content in the sediment pores.

OM source quantity and quality differed significantly between zones: The higher Biological index (BIX) and Fluorescence Index (FIX) (Table S3) in the inner zones A and B during the initial exposed phase indicate that more labile, autochthonous OM has been recently added to the OM pool compared to the outer zone C. This could be explained by a higher recent algal production (Wyatt et al., 2014). Furthermore, exposure to UV-radiation can also increase the production of labile OM fractions by degrading recalcitrant components (Paul et al., 2012; Feng et al., 2011). Additionally, fine and labile OM particles could also have been transported from the outer zone C towards the inner zones A and B (see above). Microbial exudation of labile OM compounds due to water stress (Kaiser et al., 2015; Ruiz-González et al., 2013; Schimel et al., 2007) might not have been important here, as zones A and B have not been desiccated after the dry fall. The lower abundance and also more refractory character (Fig. 4) of OM in zone C compared to the inner zones A and B seems to be determined by the hydrological history of the sediment. Extended dry periods, which are characteristic for zone C, are able to enhance microbial decomposition of labile OM due to sediment oxygenation (Nitzsche et al., 2017; Reverey et al., 2016; Weise et al., 2016; see also 4.4) as well as photochemical transformation of OM (Feng et al., 2011).

4.2. Microbial community dynamics

Direct lethal effects of desiccation on microorganisms are likely to be minor, as the water content of the sediment did not drop below 80% (zones A and B) and 60% (zone C) (Table S2). It is more likely that impacts of dry-wet cycling on the redox potential as well as other boundary conditions such as sediment texture, pH, OM quality and quantity have influenced the microbial community structure.

Bacterial abundance did not differ significantly between zones (Table 2). Fungal abundance was negatively correlated with sediment pH (Fig. 8a), which was significantly lowest in zone B (Table S2) and thus led to a higher fungal:bacterial ratio than in zones A and C (Table 2). In general, fungi have been shown to be tolerant to low pH values (Rousk et al., 2010). The pH value of lake sediments was observed to decrease after dry periods due to the oxidation of sulfide minerals (Mosley et al., 2014; Yan et al., 1996). This goes in line with our results showing a lower pH value in combination with higher sulfate concentrations during exposed conditions compared to inundated conditions in all three zones.

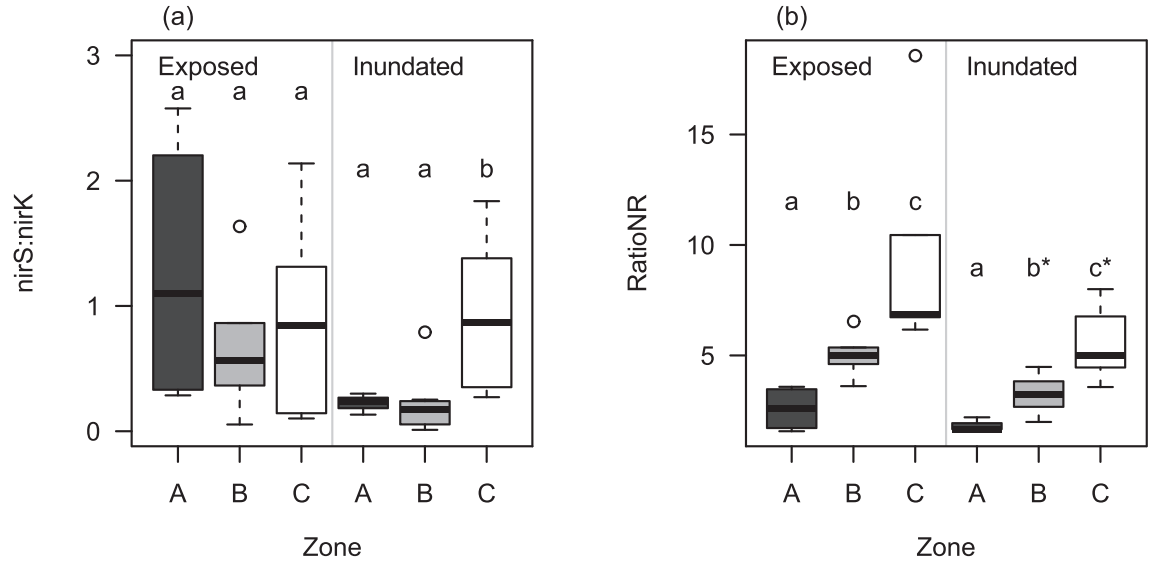

Fig. 6. (a) The ratio between gene copies for *nirS* and *nirK*. (b) The ratio between gene copies for denitrifiers (*nirS* + *nirK*) and nitrate ammonifiers (*nrfA*) (RatioNR) during exposed and inundated conditions in the three different zones. Small letters indicate significance within treatment (separated by grey line); asterisks indicate significant effects of the treatment within zones.

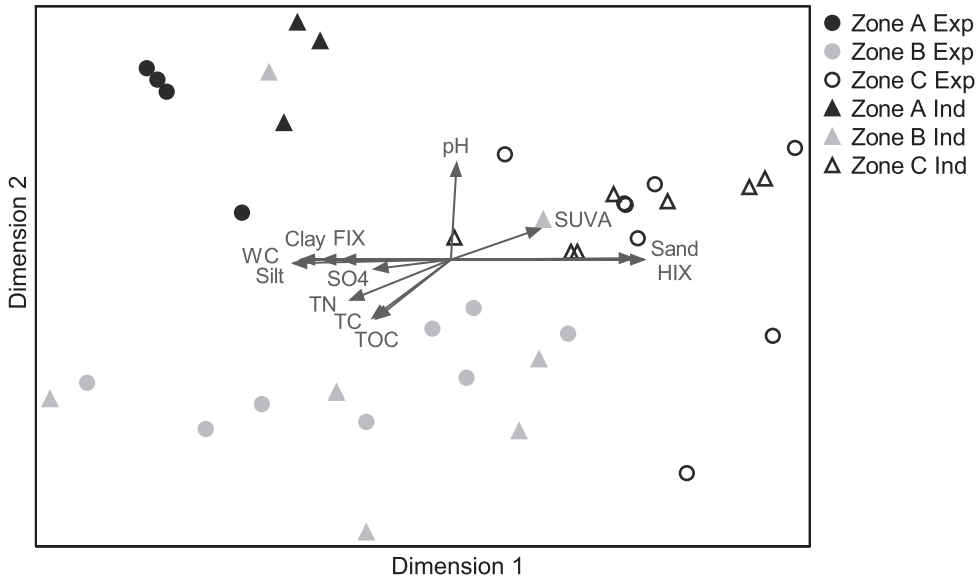

Fig. 7. NMDS ordination plot depicting the shifts in the nitrate ammonifier community of the three zones during exposed (Exp) and inundated (Ind) conditions. The analysis is based on length polymorphisms of the *nrfA* gene. The first two dimensions are displayed. Arrows indicate the correlations of abiotic descriptors with the respective dimensions ($R^2 > 0.2$).

Shifts in functional guilds became obvious in the bacterial community containing functional genes for nitrite reductase. The abundance of *nirS* was constantly lowest in zone B (Table 3), which might be explained by pH values lower than 5 (Table S2). In previous studies, the expression of the *nirS* gene was shown to be significantly impaired when the pH drops below 5 (Saleh-Lakha et al., 2009). Therefore, bacteria containing the *nirS* gene might be suppressed in environments with low pH values. Though *nirK* did not differ between the zones (Table 3), the ratio between *nirS* and *nirK* was significantly highest in the outermost zone C during inundated conditions (Fig. 6a). Bacteria expressing *nirK* are assumed to have an advantage over those expressing *nirS* in environments with high OM content, and vice versa (Bárta et al., 2010). Likewise, high TOC values can increase the importance of *nirK* compared to *nirS* (Kandeler et al., 2006). In our study, higher OM content in the inner zones A and B (Table S2) seem to drive the dominance of *nirK* over *nirS*, which is reflected in the lower values of the ratio *nirS:nirK*.

In zone A, the abundance of *nrfA*-containing bacteria was significantly highest (Table 3), thus explaining the low values of ratioNR, which indicates whether the microbial potential is more on the side of denitrification (high values) or nitrate ammonification (DNRA; low values). A higher potential for DNRA in the moister zone A than in the drier zone C suggests that DNRA is sensitive to drying. Therefore, the community of *nrfA*-containing bacteria is potentially displaying a quantitative as well as compositional change. Accordingly, the *nrfA* gene length polymorphism revealed that the communities of *nrfA*-containing bacteria were distinct in all three zones (Fig. 7). Correlations of the dimensions of the NMDS with abiotic parameters indicated that the outermost zone C mainly separated from the inner zones A and B due to the

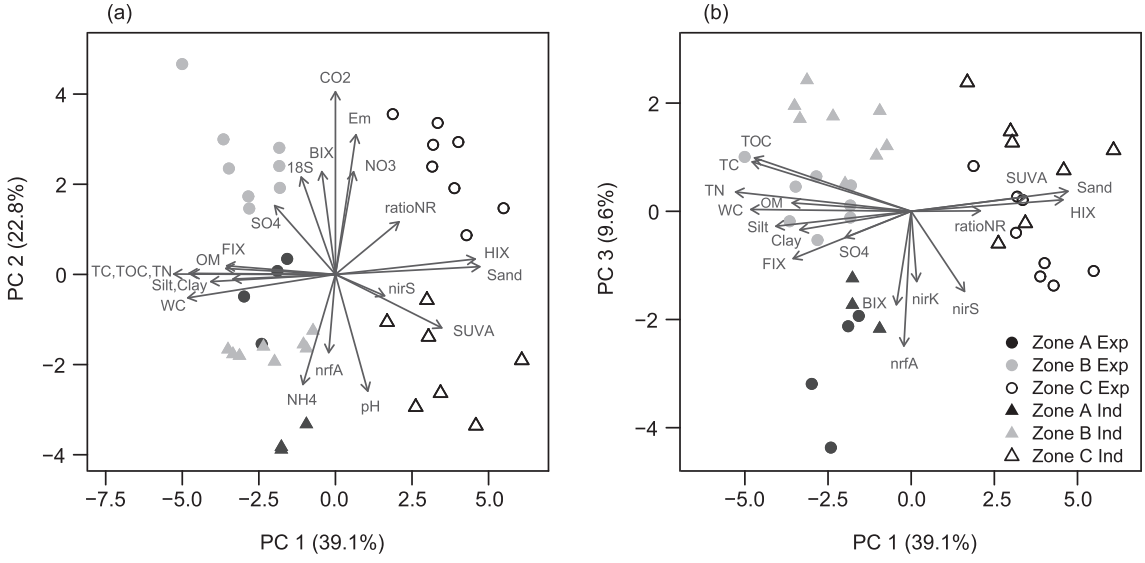

Fig. 8. Multivariate ordination (PCA) of the three zones during exposed (Exp) and inundated (Ind) conditions based on biogeochemical and microbial descriptors. The percentage of explained variance of each principal component (PC) is given in brackets. Arrows depict the correlation of each descriptor ($R^2 > 0.2$) with the respective PCs. (a) Scores of the first two PCs, (b) Scores of PC 1 and 3.

higher sand and lower water content as well as the more humic character of OM. Water content, which is related to sediment texture, has a strong effect on the redox potential of the sediment. Accordingly, sand content and lability of OM (Schmidt et al., 2011), as well as the redox state (Matheson et al., 2002), have been shown to be important factors influencing DNRA activity, therefore shaping the responsible microbial community. Furthermore, zone B was distinct from zone A mainly due to a lower pH and higher organic carbon content, which both have been shown to be important regulators of DNRA activity (Song et al., 2014; Schmidt et al., 2011). The scores of the NMDS (Fig. 7) correlate positively with the scores of principal components 1 and 3 (Fig. 8b), indicating a corresponding clustering of both ordinations. Conclusively, the hydrological history of the sediment, which is reflected in the distinctness of the zones, is driving the changes in the nitrate ammonifier community structure.

4.3. Nitrogen turnover

The potential for denitrification was always higher than that of nitrate ammonification (DNRA) in all zones, as indicated by values of RatioNR exceeding 1. Accordingly, DNRA is assumed to account for only 5–15% of total nitrate reduction in temperate freshwater systems (Sgouridis et al., 2011). Additionally, RatioNR showed an increase from zone A to zone C and thus a positive relation with the extent of previous dry periods (Fig. 6b). This notion is reflected by the positive correlation of RatioNR with PC1 (Fig. 8) and indicates a higher potential for DNRA in sediments less exposed to drought. DNRA as well as denitrification largely depend on the availability of labile carbon as electron donor, whereat DNRA is assumed to be promoted by nitrate limiting conditions and denitrification is favored in environments rich in nitrate (Sgouridis et al., 2011; Burgin and Hamilton, 2007). In combination with a lower RatioNR, this hints at a higher potential for DNRA in zone A, where labile OM was abundant and nitrate concentrations were low in the exposed phase. In zone B, co-occurrence of nitrate and labile OM during sediment exposure likely promoted denitrification, which, however, might have been inhibited by sediment oxygenation owing to longer exposure to the atmosphere. In zone C, low fractions of labile OM and high sediment oxygenation during dry conditions provided unfavorable conditions for denitrification as well as DNRA, potentially explaining the observed nitrate accumulation. Results indicate that hydrological instability decreases the potential for N retention due to DNRA.

In zones B and C, nitrate was still abundant in the exposed phase, whereas ammonium was depleted (Fig. 5). This is likely owing to the fact that ammonium was rapidly nitrified to nitrate, which accumulated due to sediment oxygenation and therefore low activity of denitrifiers and nitrate ammonifiers. This has also been observed, e.g., in wetland sediments (Akatsuka and Mitamura, 2011). On the contrary, ammonium accumulation coupled to nitrate depletion in the exposed phase further point at DNRA in zone A. It is likely that the redox potential was still low due to high water and clay content and shorter duration of the exposed phase, thus hampering nitrification and enabling DNRA.

An increase of ammonium after rewetting, in combination with decreasing nitrate concentrations, could have been expected, assuming impaired nitrification and enhanced denitrification due to a decrease in redox potential. The decrease of ammonium towards the more frequently exposed zone C (Fig. 5B) might be explained by a higher sediment oxygenation due to longer exposure to the atmosphere resulting in a more active nitrifying microbial community. In this scenario, the accumulating ammonium mainly originates from OM mineralization. However, we found a significant drop in OM lability and mineralization efficiency after rewetting in all three zones. An alternative scenario explaining the increase of ammonium coupled to a decrease of nitrate is the presence of DNRA (Arce et al., 2015). The positive correlation of *nrfA* and NH_4 (Fig. 8a), the decrease of RatioNR as well as depletion of nitrate following rewetting would support this scenario.

4.4. Carbon turnover

Mean CO_2 efflux from sediments exposed to the atmosphere was highest in zones with an antecedent exposed phase exceeding three months (i.e. zones B and C) (Fig. 3a). Previous studies have indicated a slowdown of mineralization activity with ongoing desiccation, presumably due to impaired microbial activity (Fromin et al., 2010). However, the sediment water content in the aforementioned study decreased to <40%, whereas the water content in this study did not drop below 60%. Therefore, the positive effect of exposure to air on mineralization rates might have prevailed throughout the exposed phase irrespective of its length. Furthermore, the more labile, autochthonous character of OM in zones A and B in the exposed phase, as indicated by higher values of FIX and BIX (Table S3 and Fig. 4), has the potential to promote mineralization, which contradicts the lower mineralization efficiency in zone A and B when compared to zone C (Fig. 3b). This is likely due to a stronger aeration of zone C sediment, facilitated by the lower water and higher sand content. Sediment oxygenation increases the ratio of aerobic to anaerobic mineralization, which enhances mineralization efficiency, especially in sediments containing older, more refractory OM (Hulthe et al., 1998). As zone C displayed the highest values of SUVA and HIX (indicators of aromaticity and degree of humification, respectively) (Table S2 and S3), this indicates a more efficient mineralization of rather refractory OM during dry, oxygenated conditions.

Mean CO_2 efflux was lower in zone A than in zone B, though sediment texture, OM quantity and quality did not differ significantly between both. The contribution of fungi might have enhanced CO_2 production under exposed conditions, as shown by a positive correlation of 18S rRNA gene abundance and CO_2 efflux (Fig. 8a). This seems to be particularly the case in zone B where the fungal:bacterial ratio was highest (Table 2), potentially explaining the higher measured CO_2 efflux.

Higher CO_2 production in zone B might be also due to "nitrogen mining" where microbes can use labile carbon to access nitrogen from recalcitrant sources (such as lignocellulose and humics) under nitrogen limiting conditions (Craine et al., 2007). Contrary to the basic stoichiometric decomposition theory which states a lower carbon storage if C:N ratios decrease (e.g. Mack et al., 2004), nitrogen mining thus leads to an increase of carbon mineralization when C:N ratios increase. This can be regarded a positive priming effect, where the availability of labile OM facilitates N utilization from recalcitrant sources at a high C cost (Kuzyakov, 2010). As zone B had a higher C:N ratio than zone A (i.e. 11.2 vs. 9.5, respectively; Table S2) and labile C is sufficiently abundant, this may explain the higher observed C-respiration.

Carbon mineralization efficiency significantly dropped after rewetting (Fig. 3b), which is in line with previous studies for lake sediments (Weise et al., 2016) and wetlands (Chimner and Cooper, 2003). This might be due to a combination of different effects: The amount of fresh and labile autochthonous OM was significantly lower at the end of the incubation, as indicated by decreasing values of FIX and BIX (Table S3 and Fig. 4). As the sediment was incubated in the dark, primary production could not fuel the autochthonous, labile OM pool. Therefore, labile OM which has been mineralized throughout the incubation might have become a limiting factor. Under these conditions, a drop of the redox potential after rewetting is very likely to have decreased mineralization (Hulthe et al., 1998), particularly in zone C. In zone B, a significantly decreased ratio of fungal:bacterial abundance after rewetting (Table 2) might have impaired mineralization.

Differences of mineralization efficiency between the zones disappeared during the inundated phase (Fig. 3b). Therefore, the microbial effect seems to be more on the functional level and reversible. Whether it also affected the structural level, that is, changing the microbial community to a new equilibrium, cannot be inferred from our data except for the observed differences in fungal abundance which are likely to reflect a microbial legacy of dry-wet cycling with a potential to influence carbon mineralization.

CH_4 efflux was generally low (Fig. 3a) compared to values from the growing season 2014, when the sediment was inundated and exhibited a mean CH_4 efflux of 208 ± 112 mg C m^{-2} d^{-1} (Reverey et al., 2016). Low net methane production is commonly observed as a response to drought due to an increase of redox potential (Knorr and Blodau, 2009; Megonigal et al., 2004). However, methanogenic populations have been found to be structurally less affected by redox changes, but become inactive during aeration due to substrate competition with other microorganisms (Angel et al., 2012; Yuan et al., 2009). Likewise, the accumulation of sulfate in all three zones during the exposed phase is likely to stimulate sulfate reduction, which is assumed to suppress methanogenesis (Dowrick et al., 2006). Furthermore, values of net CH_4 production during the exposed phase partly dropped to negative values, thus pointing at aerobic methane oxidation due to higher oxygenation of the sediments. As we observed no significant sediment desiccation in zones A and B, the redox potential likely increased only at the sediment surface, where methane oxidation might have eliminated the methane produced in the deeper layers. Another reason for a low net methane production could be anaerobic methane oxidation facilitated by the abundance of sulfate and nitrate that are known as alternative terminal electron acceptors (Haroon et al., 2013; Schubert et al., 2011).

5. Conclusions

Our study shows that variations in the duration and frequency of previous dry-wet events create distinct microbial habitats within kettle hole sediments with defined boundary conditions reflected by microbial community structure and specific sediment characteristics. The effect of drying on the water content, which is mainly determined by sediment texture, is less pronounced than the effect on redox sensitive processes in the investigated kettle hole. A biogeochemical legacy of dry-wet cycling seems to be mainly reflected by variations in pH as well as OM quantity and quality, which in turn, together with changes in redox conditions, have an influence on microbial diversity and function.

A high degree of lability as well as a high C:N ratio of OM promote C and N mineralization. Increased duration and frequency of previous dry-wet events decrease the OM content and increase its recalcitrant fraction, most likely due to boosted biotic and abiotic mineralization during dry phases. Lower pH values coupled with increased sulfate concentrations during exposed conditions point to oxidation of sulfuric compounds, thus producing sulfuric acid and thereby changing habitat conditions (i.e. pH), which shape microbial community structure and function.

Furthermore, the potential for denitrification was always higher than that for nitrate ammonification (DNRA). However, the hydrological history can influence the abundance of responsible functional guilds, i.e. *nirS*, *nirK* and *nrfA* containing bacteria. The retention of nitrogen in the system seems to be controlled by DNRA, but its importance in comparison to N loss due to denitrification is largely determined by the availability of nitrate and labile OM and might be impaired by previous long and reoccurring dry-wet events. Nitrate ammonifiers differed significantly between the zones and thus indicate adaptation to the specific environmental conditions. Yet, the direct link between compositional responses to dry-wet cycling and the activity level remains to be evaluated.

Conclusively, long and frequent drought events increase the potential for biotic as well as abiotic carbon mineralization and denitrification in sediments and decrease the potential for N retention via nitrate ammonification. Therefore, considering the biogeochemical legacy of dry-wet cycling is of great importance when predicting ecological and biogeochemical consequences of possible future climate change scenarios on carbon and nutrient cycling in landscapes with high numbers of temporary, small water bodies.

Acknowledgements

We would like to thank Gabriela Onandia, Carlos Miguel Acame Poveda, Katja Felsmann and Robert Hommel for their much appreciated assistance in the field and in the laboratory. Furthermore, we thank Jeremy Fonvielle and Nuria Catalan for their support with water extractions and fluorescence measurements. Additionally, we acknowledge Sigune Weinert for technical assistance in the molecular biological laboratory. This study was co-funded by the Leibniz-Centre for Agricultural Landscape Research (ZALF), the Leibniz-Institute of Freshwater Ecology and Inland Fisheries (IGB) and two projects of the Pact for Innovation and Research of the Gottfried Wilhelm Leibniz Association (project LandScales - 'Connecting processes and structures driving landscape carbon dynamics over scales' (SAW-2012-ZALF-3) and project Mycolink – 'Linking aquatic mycodiversity to ecosystem function' (SAW-2014-IGB)). HPG was further supported by the DFG project "MicroPrime" (GR1540/23-1).

Appendix A. Supplementary data

Supplementary data to this article can be found online at https://doi.org/10.1016/j.scitotenv.2018.01.220.

References

Akatsuka, T., Mitamura, O., 2011. Response of denitrification rate associated with wetting and drying cycles in a littoral wetland area of Lake Biwa, Japan. Limnology 12: 127–135. https://doi.org/10.1007/s10201-010-0329-x.

Anesio, A.M., Theil-Nielsen, J., Granéli, W., 2000. Bacterial growth on photochemically transformed leachates from aquatic and terrestrial primary producers. Microb. Ecol. 40, 200–208.

Angel, R., Claus, P., Conrad, R., 2012. Methanogenic archaea are globally ubiquitous in aerated soils and become active under wet anoxic conditions. ISME J. 6:847–862. https://doi.org/10.1038/ismej.2011.141.

Arce, M.I., Sánchez-Montoya, M.D.M., Gómez, R., 2015. Nitrogen processing following experimental sediment rewetting in isolated pools in an agricultural stream of a semiarid region. Ecol. Eng. 77:233–241. https://doi.org/10.1016/j.ecoleng.2015.01.035.

Bárta, J., Melichová, T., Vaněk, D., Picek, T., Šantrůčková, H., 2010. Effect of pH and dissolved organic matter on the abundance of nirK and nirS denitrifiers in spruce forest soil. Biogeochemistry 101:123–132. https://doi.org/10.1007/s10533-010-9430-9.

Barthès, A., Ten-Hage, L., Lamy, A., Rols, J.L., Leflaive, J., 2015. Resilience of aggregated microbial communities subjected to drought – small-scale studies. Microb. Ecol. 70: 9–20. https://doi.org/10.1007/s00248-014-0532-0.

Becker, R., Bubner, B., Remus, R., Wirth, S., Ulrich, A., 2014. Impact of multi-resistant transgenic Bt maize on straw decomposition and the involved microbial communities. Appl. Soil Ecol. 73:9–18. https://doi.org/10.1016/j.apsoil.2013.08.002.

Burgin, A.J., Hamilton, S.K., 2007. Have we overemphasized the role of denitrification in aquatic ecosystems? A review of nitrate removal pathways. Front. Ecol. Environ. 5: 89–96. https://doi.org/10.1890/1540-9295(2007)5[89:HWOTRO]2.0.CO;2.

Catalan, N., von Schiller, D., Marce, R., Koschorreck, M., Gomez-Gener, L., Obrador, B., 2014. Carbon dioxide efflux during the flooding phase of temporary ponds. Limnetica 33, 349–359.

Chimner, R.A., Cooper, D.J., 2003. Carbon dynamics of pristine and hydrologically modified fens in the southern Rocky Mountains. Can. J. Bot. 81:477–491. https://doi.org/10.1139/b03-043.

Cory, R.M., McKnight, D.M., 2005. Fluorescence spectroscopy reveals ubiquitous presence of oxidized and reduced quinones in dissolved organic matter. Environ. Sci. Technol. 39:8142–8149. https://doi.org/10.1021/es0506962.

Craine, J.M., Morrow, C., Fierer, N., 2007. Microbial nitrogen limitation increases decomposition. Ecology 88:2105–2113. https://doi.org/10.1890/06-1847.1.

DeAngelis, K.M., Silver, W.L., Thompson, A.W., Firestone, M.K., 2010. Microbial communities acclimate to recurring changes in soil redox potential status. Environ. Microbiol. 12:3137–3149. https://doi.org/10.1111/j.1462-2920.2010.02286.x.

Dinno, A., 2016. Dunn Test: Dunn's Test of Multiple Comparisons Using Rank Sums. R Package Version 1.3.2. http://CRAN.R-project.org/package=dunn.test.

Dowrick, D.J., Freeman, C., Lock, M.A., Reynolds, B., 2006. Sulphate reduction and the suppression of peatland methane emissions following summer drought. Geoderma 132: 384–390. https://doi.org/10.1016/j.geoderma.2005.06.003.

Dray, S., Dufour, A.B., 2007. The ade4 package: implementing the duality diagram for ecologists. J. Stat. Softw. 22:1–20. https://doi.org/10.18637/jss.v022.i04.

Dunbar, J., Ticknor, L.O., Kuske, C.R., 2001. Phylogenetic specificity and reproducibility and new method for analysis of terminal restriction fragment profiles of 16S rRNA genes from bacterial communities. Appl. Environ. Microbiol. 67:190–197. https://doi.org/10.1128/AEM.67.1.190-197.2001.

Evans, S.E., Wallenstein, M.D., 2011. Soil microbial community response to drying and rewetting stress: does historical precipitation regime matter? Biogeochemistry 109: 101–116. https://doi.org/10.1007/s10533-011-9638-3.

Fabian, J., Zlatanovic, S., Mutz, M., Premke, K., 2017. Fungal-bacterial dynamics and their contribution to terrigenous carbon turnover in relation to organic matter quality. ISME J. 11:415–425. https://doi.org/10.1038/ismej.2016.131.

Felsmann, K., Baudis, M., Gimbel, K., Kayler, Z.E., Ellerbrock, R., Bruelheide, H., Bruckhoff, J., Welk, E., Puhlmann, H., Weiler, M., Gessler, A., Ulrich, A., 2015. Soil bacterial community structure responses to precipitation reduction and forest management in forest ecosystems across Germany. PLoS ONE 10, e0122539. https://doi.org/10.1371/journal.pone.0127608.

Feng, X., Hills, K.M., Simpson, A.J., Whalen, J.K., Simpson, M.J., 2011. The role of biodegradation and photo-oxidation in the transformation of terrigenous organic matter. Org. Geochem. 42:262–274. https://doi.org/10.1016/j.orggeochem.2011.01.002.

Fischer, E.M., Knutti, R., 2015. Anthropogenic contribution to global occurrence of heavy-precipitation and high-temperature extremes. Nat. Clim. Chang. 5:560–564. https://doi.org/10.1038/nclimate2617.

Fromin, N., Pinay, G., Montuelle, B., Landais, D., Ourcival, J.M., Joffre, R., Lensi, R., 2010. Impact of seasonal sediment desiccation and rewetting on microbial processes involved in greenhouse gas emissions. Ecohydrology 3:339–348. https://doi.org/10.1002/Eco.115.

Goldenfum, J.A., 2010. GHG measurement guidelines for freshwater reservoirs. Sutton, London: Derived from: The UNESCO/IHA Greenhouse Gas Emission from Freshwater Reservoirs Research Project. International Hydropower Association.

Gómez-Gener, L., Obrador, B., Marcé, R., Acuña, V., Catalán, N., Casas-Ruiz, J.P., Sabater, S., Muñoz, I., Schiller, D., 2016. When water vanishes: magnitude and regulation of carbon dioxide emissions from dry temporary streams. Ecosystems 19:710–723. https://doi.org/10.1007/s10021-016-9963-4.

Haroon, M.F., Hu, S., Shi, Y., Imelfort, M., Keller, J., Hugenholtz, P., Yuan, Z., Tyson, G.W., 2013. Anaerobic oxidation of methane coupled to nitrate reduction in a novel archaeal lineage. Nature 500:567–570. https://doi.org/10.1038/nature12375.

Henry, S., Baudoin, E., López-Gutiérrez, J.C., Martin-Laurent, F., Brauman, A., Philippot, L., 2004. Quantification of denitrifying bacteria in soils by nirK gene targeted real-time PCR. J. Microbiol. Methods 59:327–335. https://doi.org/10.1016/j.mimet.2004.07.002.

Hillel, D., 1980. Soil water: content and potential. Fundamentals of Soil Physics. Academic Press, San Diego:pp. 123–165 https://doi.org/10.1016/B978-0-08-091870-9.50012-1.

Huguet, A., Vacher, L., Relexans, S., Saubusse, S., Froidefond, J.M., Parlanti, E., 2009. Properties of fluorescent dissolved organic matter in the Gironde estuary. Org. Geochem. 40:706–719. https://doi.org/10.1016/j.orggeochem.2009.03.002.

Hulthe, G., Hulth, S., Hall, P.O.J., 1998. Effect of oxygen on degradation rate of refractory and labile organic matter in continental margin sediments. Geochim. Cosmochim. Acta 62:1319–1328. https://doi.org/10.1016/S0016-7037(98)00044-1.

Kaiser, M., Kleber, M., Berhe, A.A., 2015. How air-drying and rewetting modify soil organic matter characteristics: an assessment to improve data interpretation and inference. Soil Biol. Biochem. 80:324–340. https://doi.org/10.1016/j.soilbio.2014.10.018.

Kalettka, T., Rudat, C., 2006. Hydrogeomorphic types of glacially created kettle holes in North-East Germany. Limnologica 36:54–64. https://doi.org/10.1016/j.limno.2005.11.001.

Kandeler, E., Deiglmayr, K., Tscherko, D., Bru, D., Philippot, L., 2006. Abundance of narG, nirS, nirK, and nosZ genes of denitrifying bacteria during primary successions of a glacier foreland. Appl. Environ. Microbiol. 72:5957–5962. https://doi.org/10.1128/AEM.00439-06.

Kaplan, C.W., Kitts, C.L., 2003. Variation between observed and true terminal restriction fragment length is dependent on true TRF length and purine content. J. Microbiol. Methods 54:121–125. https://doi.org/10.1016/S0167-7012(03)00003-4.

Kleeberg, A., Neyen, M., Schkade, U.K., Kalettka, T., Lischeid, G., 2016. Sediment cores from kettle holes in NE Germany reveal recent impacts of agriculture. Environ. Sci. Pollut. Res. 23:7409–7424. https://doi.org/10.1007/s11356-015-5989-y.

Knorr, K.H., Blodau, C., 2009. Impact of experimental drought and rewetting on redox transformations and methanogenesis in mesocosms of a northern fen soil. Soil Biol. Biochem. 41:1187–1198. https://doi.org/10.1016/j.soilbio.2009.02.030.

Knorr, K.H., Oosterwoud, M.R., Blodau, C., 2008. Experimental drought alters rates of soil respiration and methanogenesis but not carbon exchange in soil of a temperate fen. Soil Biol. Biochem. 40:1781–1791. https://doi.org/10.1016/j.soilbio.2008.03.019.

Kuzyakov, Y., 2010. Priming effects: interactions between living and dead organic matter. Soil Biol. Biochem. 42:1363–1371. https://doi.org/10.1016/j.soilbio.2010.04.003.

Mack, M.C., Schuur, E.A.G., Bret-Harte, M.S., Shaver, G.R., Chapin, F.S., 2004. Ecosystem carbon storage in arctic tundra reduced by long-term nutrient fertilization. Nature 431:440–443. https://doi.org/10.1038/nature02887.

Matheson, F.E., Nguyen, M.L., Cooper, A.B., Burt, T.P., Bull, D.C., 2002. Fate of ^{15}N-nitrate in unplanted, planted and harvested riparian wetland soil microcosms. Ecol. Eng. 19:249–264. https://doi.org/10.1016/S0925-8574(02)00093-9.

McCune, B., Mefford, M.J., 2015. PC-ORD. Multivariate Analysis of Ecological Data. 7.0 ed. MjM Software, Gleneden Beach, Oregon, U.S.

Megonigal, J.P., Hines, M.E., Visscher, P.T., 2004. Anaerobic Metabolism: Linkages to Trace Gases and Aerobic Processes, Treatise on Geochemistry. Second edition. pp. 273–359.

Mosley, L.M., Zammit, B., Jolley, A.M., Barnett, L., 2014. Acidification of lake water due to drought. J. Hydrol. 511:484–493. https://doi.org/10.1016/j.jhydrol.2014.02.001.

Murphy, K.R., Butler, K.D., Spencer, R.G.M., Stedmon, C.A., Boehme, J.R., Aiken, G.R., 2010. Measurement of dissolved organic matter fluorescence in aquatic environments: an interlaboratory comparison. Environ. Sci. Technol. 44:9405–9412. https://doi.org/10.1021/es102362t.

Nercessian, O., Noyes, E., Kalyuzhnaya, M.G., Lidstrom, M.E., Chistoserdova, L., 2005. Bacterial populations active in metabolism of C1 compounds in the sediment of Lake Washington, a freshwater lake. Appl. Environ. Microbiol. 71:6885–6899. https://doi.org/10.1128/AEM.71.11.6885-6899.2005.

Nitzsche, K.N., Kalettka, T., Premke, K., Lischeid, G., Gessler, A., Kayler, Z.E., 2017. Land-use and hydroperiod affect kettle hole sediment carbon and nitrogen biogeochemistry. Sci. Total Environ. 574:46–56. https://doi.org/10.1016/j.scitotenv.2016.09.003.

Paul, A., Dziallas, C., Zwirnmann, E., Gjessing, E.T., Grossart, H.P., 2012. UV irradiation of natural organic matter (NOM): impact on organic carbon and bacteria. Aquat. Sci. 74:443–454. https://doi.org/10.1007/s00027-011-0239-y.

Peralta, A.L., Ludmer, S., Kent, A.D., 2013. Hydrologic history influences microbial community composition and nitrogen cycling under experimental drying/wetting treatments. Soil Biol. Biochem. 66:29–37. https://doi.org/10.1016/j.soilbio.2013.06.019.

Peralta, A.L., Matthews, J.W., Kent, A.D., 2014. Habitat specialization along a wetland moisture gradient differs between ammonia-oxidizing and denitrifying microorganisms. Microb. Ecol. 68:339–350. https://doi.org/10.1007/s00248-014-0407-4.

R Core Team, 2014. R: A Language and Environment for Statistical Computing. R Foundation for Statistical Computing, Vienna, Austria URL. http://www.R-project.org/.

Reiche, M., Hädrich, A., Lischeid, G., Küscl, K., 2009. Impact of manipulated drought and heavy rainfall events on peat mineralization processes and source-sink functions of an acidic fen. J. Geophys. Res. Biogeosci. 114, G02021. https://doi.org/10.1029/2008JG000853.

Reverey, F., Grossart, H.P., Premke, K., Lischeid, G., 2016. Carbon and nutrient cycling in kettle hole sediments depending on hydrological dynamics: a review. Hydrobiologia 775:1–20. https://doi.org/10.1007/s10750-016-2715-9.

Rousk, J., Bååth, E., Brookes, P.C., Lauber, C.L., Lozupone, C., Caporaso, J.G., Knight, R., Fierer, N., 2010. Soil bacterial and fungal communities across a pH gradient in an arable soil. ISME J. 4:1340–1351. https://doi.org/10.1038/ismej.2010.58.

Ruiz-González, C., Simó, R., Sommaruga, R., Gasol, J.M., 2013. Away from darkness: a review on the effects of solar radiation on heterotrophic bacterioplankton activity. Front. Microbiol. 4. https://doi.org/10.3389/fmicb.2013.00131.

Saleh-Lakha, S., Shannon, K.E., Henderson, S.L., Goyer, C., Trevors, J.T., Zebarth, B.J., Burton, D.L., 2009. Effect of pH and temperature on denitrification gene expression and activity in *Pseudomonas mandelii*. Appl. Environ. Microbiol. 75:3903–3911. https://doi.org/10.1128/AEM.00080-09.

Schimel, J., Balser, T.C., Wallenstein, M., 2007. Microbial stress-response physiology and its implications for ecosystem function. Ecology 88:1386–1394. https://doi.org/10.1890/06-0219.

Schmidt, C.S., Richardson, D.J., Baggs, E.M., 2011. Constraining the conditions conducive to dissimilatory nitrate reduction to ammonium in temperate arable soils. Soil Biol. Biochem. 43:1607–1611. https://doi.org/10.1016/j.soilbio.2011.02.015.

Schubert, C.J., Vazquez, F., Lösekann-Behrens, T., Knittel, K., Tonolla, M., Boetius, A., 2011. Evidence for anaerobic oxidation of methane in sediments of a freshwater system (Lago di Cadagno). FEMS Microbiol. Ecol. 76:26–38. https://doi.org/10.1111/j.1574-6941.2010.01036.x.

Sgouridis, F., Heppell, C.M., Wharton, G., Lansdown, K., Trimmer, M., 2011. Denitrification and dissimilatory nitrate reduction to ammonium (DNRA) in a temperate, re-connected floodplain. Water Res. 45:4909–4922. https://doi.org/10.1016/j.watres.2011.06.037.

Song, B., Lisa, J.A., Tobias, C.R., 2014. Linking DNRA community structure and activity in a shallow lagoonal estuarine system. Front. Microbiol. 5. https://doi.org/10.3389/fmicb.2014.00460.

Weise, L., Ulrich, A., Moreano, M., Gessler, A., Kayler, Z.E., Steger, K., Zeller, B., Rudolph, K., Knezevic-Jaric, J., Premke, K., 2016. Water level changes affect carbon turnover and microbial community composition in lake sediments. FEMS Microbiol. Ecol. 92, fiw035. https://doi.org/10.1093/femsec/fiw035.

Weishaar, J.L., Aiken, G.R., Bergamaschi, B.A., Fram, M.S., Fujii, R., Mopper, K., 2003. Evaluation of specific ultraviolet absorbance as an indicator of the chemical composition and reactivity of dissolved organic carbon. Environ. Sci. Technol. 37:4702–4708. https://doi.org/10.1021/es030360x.

Wyatt, K.H., Rober, A.R., Schmidt, N., Davison, I.R., 2014. Effects of desiccation and rewetting on the release and decomposition of dissolved organic carbon from benthic macroalgae. Freshw. Biol. 59:407–416. https://doi.org/10.1111/Fwb.12273.

Yan, N.D., Keller, W., Scully, N.M., Lean, D.R.S., Dillon, P.J., 1996. Increased UV-B penetration in a lake owing to drought-induced acidification. Nature 381:141–143. https://doi.org/10.1038/381141a0.

Yuan, Y., Conrad, R., Lu, Y., 2009. Responses of methanogenic archaeal community to oxygen exposure in rice field soil. Environ. Microbiol. Rep. 1:347–354. https://doi.org/10.1111/j.1758-2229.2009.00036.x.

Zeleke, J., Sheng, Q., Wang, J.G., Huang, M.Y., Xia, F., Wu, J.H., Quan, Z.X., 2013. Effects of *Spartina alterniflora* invasion on the communities of methanogens and sulfate-reducing bacteria in estuarine marsh sediments. Front. Microbiol. 4. https://doi.org/10.3389/fmicb.2013.00243.

Zsolnay, A., Baigar, E., Jimenez, M., Steinweg, B., Saccomandi, F., 1999. Differentiating with fluorescence spectroscopy the sources of dissolved organic matter in soils subjected to drying. Chemosphere 38:45–50. https://doi.org/10.1016/S0045-6535(98)00166-0.